Comparative X-ray Photoelectron Spectroscopic Study on the Desulfurization of Thiophene by Raney Nickel and Rapidly Quenched Skeletal Nickel

Huarong Hu,[†] Minghua Qiao,*[,†] Fuzhong Xie,[†] Kangnian Fan,*[,†] Hao Lei,[‡] Dali Tan,[‡] Xinhe Bao,[‡] Hailong Lin,[§] Baoning Zong,[§] and Xiaoxin Zhang[§]

Department of Chemistry and Shanghai Key Laboratory of Molecular Catalysis and Innovative Materials, Fudan University, Shanghai 200433, People's Republic of China, State Key Laboratory of Catalysis, Dalian Institute of Chemical Physics, Chinese Academy of Sciences, Dalian 116023, People's Republic of China, and Research Institute of Petroleum Processing, Beijing 100083, People's Republic of China

Received: October 26, 2004; In Final Form: January 4, 2005

The desulfurization of thiophene on Raney Ni and rapidly quenched skeletal Ni (RQ Ni) has been studied in ultrahigh vacuum (UHV) by X-ray photoelectron spectroscopy (XPS). The Raney Ni or RQ Ni can be approximated as a hydrogen-preadsorbed polycrystalline Ni−alumina composite. It is found that thiophene molecularly adsorbs on Raney Ni or RQ Ni at 103 K. At 173 K, thiophene on alumina is desorbed, while thiophene in direct contact with the metallic Ni in Raney Ni undergoes C−S bond scission, leading to carbonaceous species most probably in the metallocycle-like configuration and atomic sulfur. On RQ Ni, the temperature for thiophene dissociation is about 100 K higher than that on Raney Ni. The lower reactivity of RQ Ni toward thiophene is tentatively attributed to lattice expansion of Ni crystallites in RQ Ni due to rapid quenching. The existence of alumina and hydrogen may block the further cracking of the metallocycle-like species on Raney Ni and RQ Ni at higher temperatures, which has been the dominant reaction pathway on Ni single crystals. By 473 K, the C 1s peak has disappeared, leaving nickel sulfide on the surface.

1. Introduction

Most transportation fuels used nowadays contain 100−1000 ppm of organosulfur molecules. These S-containing molecules not only react with oxygen during combustion processes, producing SO_x species that lead to acid rain,[1] but also poison catalytic converters, affecting the other pollutants as well.[2,3] The European Union and United States have decided to lower sulfur in gasoline and diesel fuels to levels around 10−15 ppm in the coming years.[4−6] For fuel cells using gasoline as feedstock, it is also noted that the sulfur content below 0.2 ppm is preferred.[7]

To meet the stringent environmental regulations, considerable efforts are devoted to the development of more active hydrodesulfurization (HDS) catalysts. However, the HDS processes are not effective for thiophenic compound removal and a lot of unnecessary hydrogen is consumed, and the octane/cetane number of gasoline/diesel falls because the olefins are hydrogenated.[4] Besides, more volumetric reactor and critical reaction conditions have to be employed,[4,8] making the HDS process economically less competitive.

Desulfurization by adsorption can be a promising alternative to circumvent the shortcomings of HDS.[7−14] Molecular sieves and oxides with or without metal modifications are among the most heavily investigated adsorbents. In contrast, less attention has been paid to metallic adsorbents, although Raney Ni has seen widespread use in the desulfurization of organic and organometallic compounds.[15−17] Recently, Lin[18] systematically investigated the desulfurization of organosulfur molecules in gasoline over a series of RQ Ni/Ni−M (M = Mo, Co, Fe, and Cu) adsorbents prepared by alkaline leaching of Al from rapidly quenched Ni−Al/Ni−M−Al alloys. It is found that the desulfurization efficiency is closely related to the nature of the organosulfur molecules and the additives to the Ni−Al alloy. Skeletal Ni samples such as Raney Ni and RQ Ni have unique sponge structure and bear the merits of high surface area, high porosity, large pore size, low cost, and ready availability,[19−21] thus having the potentiality to be efficacious adsorbents for sulfur removal in clean fuel production. Moreover, since rapid quenching can lead to refined and more uniform microstructures as well as to deviations from equilibrium regarding phases and compositions, it can affect the physical and chemical properties of Raney-type adsorbents.[21−24] However, there is no surface chemistry study on the interaction of organosulfur molecules with polycrystalline Ni such as Raney Ni and RQ Ni to the best of our knowledge, yet ultrahigh vacuum studies are informative in gaining detailed insights into the fundamental aspects of desulfurization on these adsorbents, which is crucial for the design and recovery of novel sulfur removal adsorbents.

Thiophene has received extensive attention in desulfurization studies because it is more difficult to desulfurize than thiols, disulfides, or thioethers.[25,26] It is also generally regarded as representative of higher molecular weight, aromatic, organosulfur molecules in fuels.[27] In this paper, we have examined the adsorption and reaction of thiophene on Raney Ni and RQ Ni using X-ray photoelectron spectroscopy (XPS). By varying the dosages of thiophene and the temperatures of the substrates, the adsorption states and decomposition products of thiophene have been identified. The effect of the nature of the substrates on the surface chemistry of thiophene are discussed and correlated.

* Corresponding authors: e-mail mhqiao@fudan.edu.cn (M.H.Q.) and knfan@fudan.edu.cn (K.N.F.); phone 86-21-65643792; fax 86-21-65641740.
[†] Fudan University.
[‡] Dalian Institute of Chemical Physics.
[§] Research Institute of Petroleum Processing.

10.1021/jp045119z CCC: $30.25
Published on Web 02/26/2005

2. Experimental Section

2.1. Sample Preparation. The rapidly quenched $Ni_{50}Al_{50}$ alloy was prepared by a single roller melt-spinning technique. A mixture containing about equal weights of metallic Ni and metallic Al of purity higher than 99.9% was melted at 1573 K in an induction furnace for a sufficiently long time to ensure the homogeneity of the samples. The ribbon about 5 mm wide and 20 μm thick was fabricated by spraying the molten mixture to a water-cooled high-speed rotating copper wheel with a cooling rate of 10^6 K·s^{-1}. The alloy was subsequently ground with an agate mortar and the fraction of 0.0076−0.0154 cm was used for activation and surface chemistry study.

The RQ Ni sample was prepared by leaching the above Ni−Al alloy with 20 wt % NaOH solution in 4-fold excess with respect to Al by weight. The leaching time was 1 h and the leaching temperature was 363 K. The conditions were chosen in order to obtain completely and uniformly leached sample. After leaching, the black powder was washed free from alkali by distilled water and by ethanol to replace water and then stored in ethanol for test. Raney Ni catalyst was prepared by alkali leaching of a commercially available naturally cooled Ni−Al alloy (Ni/Al, 50/50 w/w, Shanghai Chemical Corp.) by the same procedure. It should be noted that as RQ Ni catalyst is pyrophoric, just like Raney Ni, during sample handling, care must be taken to preclude air oxidation.

2.2. XPS Measurement. Photoelectron studies were carried out on a LHS-12 system (Leybold AG) equipped with an X-ray source, a hemispherical electron energy analyzer (EA11/100), and an SRTD-12 sample manipulator (IGT Instrumente-und Gerate-Technik GmbH) that can be resistively heated to 1573 K and conductively cooled to 93 K. XPS spectra were acquired with Mg Kα radiation ($h\nu$ = 1253.6 eV) and 100 eV pass energy. The binding energy (BE) scale was calibrated by the Au $4f_{7/2}$ line of gold foil, Ag $3d_{5/2}$ line of silver foil and Cu $2p_{3/2}$ line of copper foil at 84.0, 368.3, and 932.7 eV, respectively, to minimize the nonlinearity of the energy analyzer.

Raney Ni or RQ Ni with storage liquid was placed on the sample holder and quickly inserted into the pretreatment chamber, in which heating/cooling of the sample and dosing of thiophene were conducted. First, the sample was degassed at 383 K to base pressure better than 1.5×10^{-7} Torr. Then it was transferred to the main chamber for argon ion sputtering and XPS measurements. After repeated heating and sputtering, metallic Ni became the predominant nickel species, signifying the effectiveness of the cleaning procedure. The clean sample was cooled to 103 K by liquid nitrogen before thiophene adsorption. Prior to dosing, thiophene (Acros, 99.5%) was purified by repeated freeze−pump−thaw cycles. Dosing was accomplished by backfilling the pretreatment chamber through a variable leak valve without gauge sensitivity calibration. During all XPS measurements, the sample was cooled to 103 K, and the base pressure of the main chamber remained better than 2×10^{-9} Torr.

3. Results

3.1. Thiophene on Raney Ni. The top panel of Figure 1 shows the S 2p spectra acquired after adsorption of thiophene on Raney Ni surface at 103 K followed by sequential annealing to elevated temperatures. The S 2p spectrum is composed of $2p_{3/2}$ and $2p_{1/2}$ peaks with an intensity ratio of 2:1, as theoretically determined from the spin−orbital splitting effect.[28] For exposure of 5 Langmuir (L; 1 L = 1×10^{-6} Torr·s), only one doublet is observed for thiophene, which is characterized by a S $2p_{3/2}$ peak at 165.1 eV. Further dosing of thiophene (20 L) does not affect the number and position of the S 2p peak but intensifies the S 2p doublet, indicating condensation of thiophene in a physisorbed multilayer.[29]

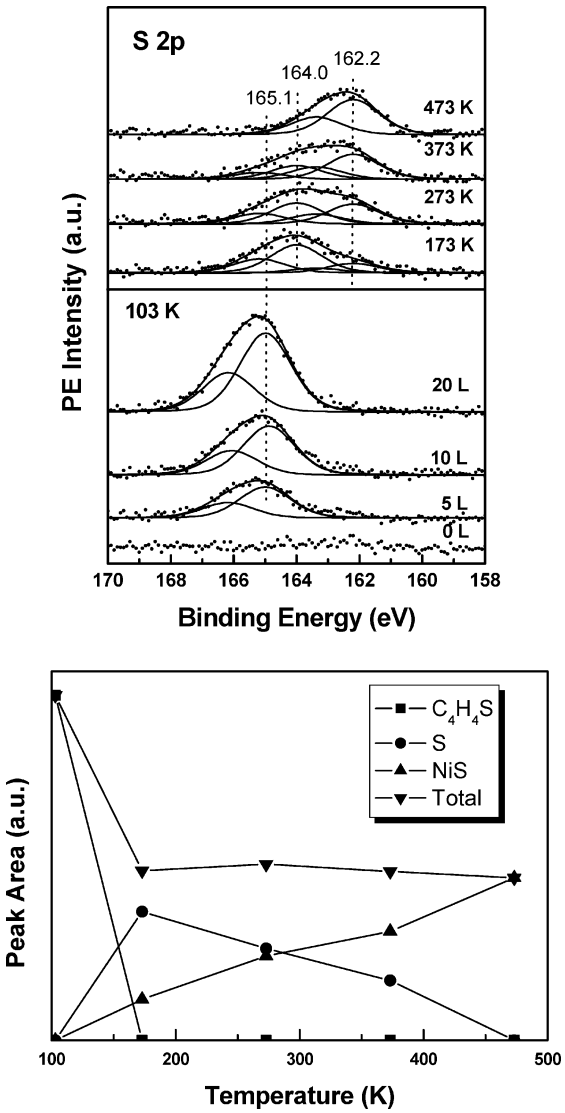

Figure 1. (Top panel) S 2p spectra for the adsorption of thiophene on a Raney Ni at 103 K, followed by annealing to 173, 273, 373, and 473 K. (Bottom panel) Integrated S $2p_{3/2}$ peak area of various sulfur species as a function of annealing temperature.

Upon annealing to 173 K, the feature due to physisorbed thiophene diminishes completely and a much broader feature appears between 160 and 167 eV, which can be well fitted into two doublets with the BEs of the S $2p_{3/2}$ levels positioned at 164.0 and 162.2 eV, representing atomic S and sulfur in nickel sulfide, respectively.[30,31] According to the bottom panel in Figure 1, which illustrates the S $2p_{3/2}$ intensity evolution versus annealing temperature, from 103 to 173 K about 51% of the physisorbed thiophene is desorbed, while ~37% undergoes C−S bond scission and ~12% further reacts with Ni to form nickel sulfide. Further annealing leads to more nickel sulfide at the expense of atomic S. At 473 K, nickel sulfide is the dominant sulfur-containing species on Raney Ni. It should be mentioned that from 173 to 473 K, no sulfur intensity loss can be found within the experimental error, suggesting that all sulfur species left on the surface are converted to nickel sulfide during the surface reaction process.

The C 1s difference spectra, taken at the same stage of the experiments in Figure 1, are shown in Figure 2. To eliminate

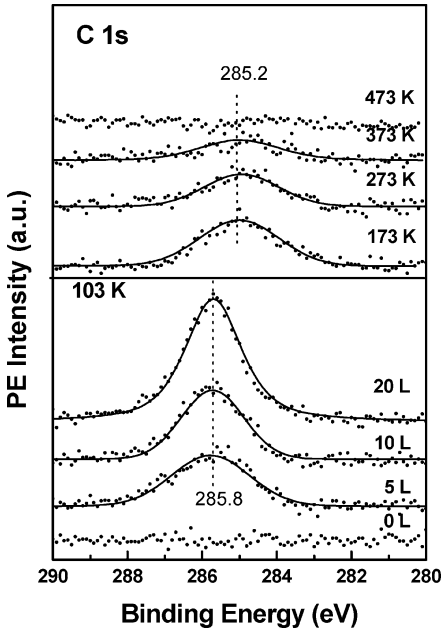

Figure 2. C 1s difference spectra for the adsorption of thiophene on a Raney Ni surface at 103 K, followed by annealing to 173, 273, 373, and 473 K. The C 1s spectrum before thiophene dosage was subtracted from these spectra.

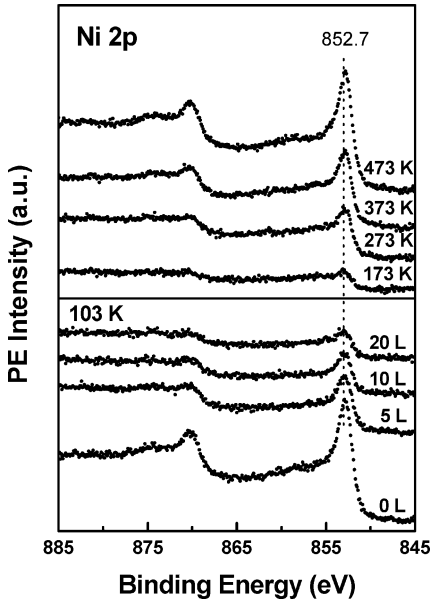

Figure 3. Ni 2p spectra for the adsorption of thiophene on a Raney Ni surface at 103 K, followed by annealing to 173, 273, 373, and 473 K.

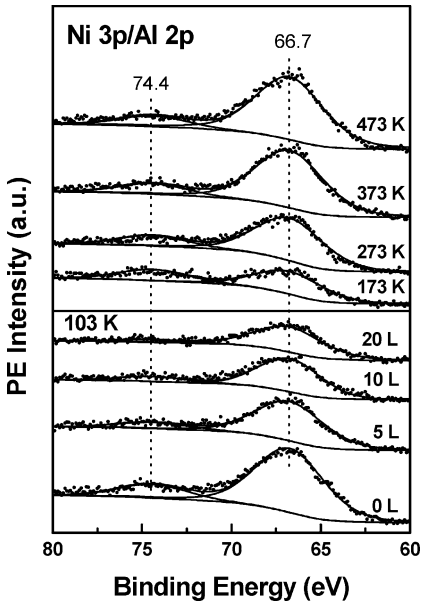

Figure 4. Ni 3p/Al 2p spectra for thiophene on Raney Ni. After a total exposure of 20 L at 103 K, the sample was annealed to 173, 273, 373, and 473 K.

the influence of contaminant carbon, the C 1s spectra before thiophene dosage was subtracted. Upon the first 5 L dose of thiophene at 103 K, a symmetric peak centered at 285.8 eV appears. Similar to the case of S 2p, the position and width of the C 1s peak remain constant upon further dosing to 20 L, while its intensity is increased. For gas-phase thiophene, Gelius et al.[32] reported a single C 1s peak at 290.4 eV relative to the vacuum level (E_v), which is intrinsically composed of two peaks of the same intensity with a binding energy separation of 0.34 $\pm$ 0.12 eV. For condensed thiophene, due to the solid-state broadening effect, with synchrotron-based high-resolution XPS only one C 1s peak at 286.0 eV relative to the Fermi level (E_F) was resolved,[29] which is in compliance with our observation.

At 173 K, the intensity of the C 1s peak is dropped to a similar extent as that of the S 2p peak, corroborating well with occurrence of the desorption of molecular thiophene. Meanwhile, the peak is negatively shifted by 0.6 eV, suggesting a stronger interaction with the substrate. Combined with the BE changes of the S 2p peak, it can be ascribed to carbonaceous species formation after sulfur abstraction. Moreover, the full width at half-maximum (fwhm) of the C 1s peak does not change as compared to that of physisorbed thiophene, inferring only one type of carbon species on Raney Ni. Unlike sulfur, the intensity of the C 1s peak decreases monotonically, and finally at 473 K the C 1s spectrum is identical to that before adsorption of thiophene.

The Ni 2p spectra are shown in Figure 3, from which one can see that Ni is solely in its metallic state in Raney Ni, as verified by the Ni $2p_{3/2}$ peak at 852.7 eV.[30] Upon dosing of thiophene at 103 K, the Ni 2p feature is attenuated, attributable to the coverage of physisorbed thiophene. Interestingly, the Ni 2p signal is further weakened upon annealing to 173 K, despite the fact that the desorption of thiophene is clearly evidenced by the S 2p and C 1s spectra, suggesting that more metallic nickel atoms on the surface are covered. At higher annealing temperatures, the Ni 2p feature gradually regains its intensity. It should be noted here that since the Ni $2p_{3/2}$ BE of nickel sulfide is 852.8 eV,[30] close to that of metallic Ni, nickel sulfide cannot be differentiated from metallic Ni even when the amount of nickel sulfide is maximum at 473 K.

Figure 4 displays the Ni 3p/Al 2p spectra, which provide additional information on the role of aluminum in Raney Ni. By deconvoluting the spectra, two peaks at ~66.7 and 74.4 eV are readily resolved, attributed to metallic Ni and Al(III) due to residual alumina in Raney Ni after alkaline leaching of aluminum in the Ni−Al alloy, respectively.[30] Both the Ni 3p and Al 2p peaks are obscured when dosed with thiophene at 103 K owing to the nonselective nature of physisorption. The evolution of the intensity of the Ni 3p peak mimics that of the Ni 2p peak, while the Al 2p peak does not: when the substrate is heated to 173 K, the intensity of the Al 2p peak resembles that of the clean surface, signifying their different reactivities toward thiophene.

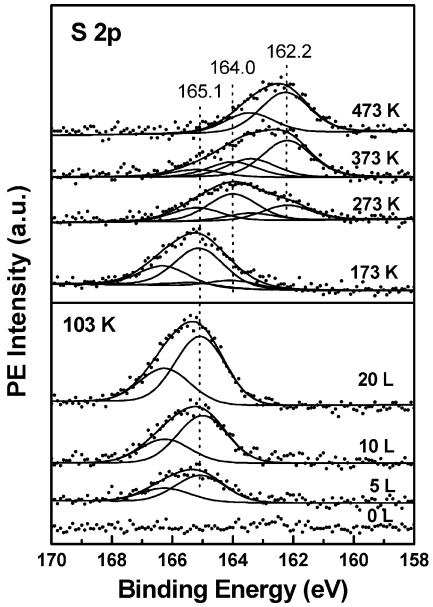

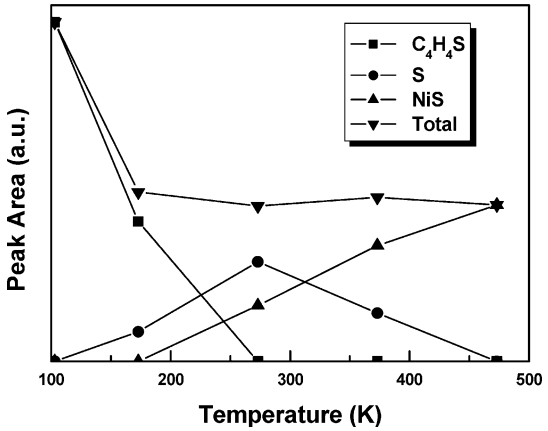

Figure 5. (Top panel) S 2p spectra for the adsorption of thiophene on a RQ Ni surface at 103 K, followed by annealing to 173, 273, 373, and 473 K. (Bottom panel) Integrated S $2p_{3/2}$ peak area of various sulfur species as a function of annealing temperature.

3.2. Thiophene on RQ Ni. Adsorption and thermal dissociation of thiophene on RQ Ni were studied in a way similar to Raney Ni. The top panel of Figure 5 shows the S 2p spectra after the adsorption of thiophene on RQ Ni surface at 103 K, followed by annealing to 173, 273, 373, and 473 K, while the bottom panel shows the corresponding S $2p_{3/2}$ intensity evolution as a function of annealing temperature. Similarly to Raney Ni, physisorbed thiophene with S $2p_{3/2}$ BE of 165.1 eV appears after dosing thiophene on RQ Ni at 103 K. After being heated to 173 K, about half of the physisorbed thiophene is desorbed. However, only ~17% of the residual thiophene undergoes sulfur abstraction, while the rest remains intact, different from the behavior on Raney Ni. Further annealing to 273 K induces the scission of the C−S bonds of residual thiophene, and the surface concentration of atomic S reaches its maximum. The formation of nickel sulfide commences at 273 K. At 473 K, there is only one doublet located between 160 and 165 eV due to sulfur in nickel sulfide. The total sulfur intensity remains constant from 173 to 473 K, which is coherent with the observation on Raney Ni.

Figure 6 is the C 1s difference spectra taken at the same stage as that in Figure 5. In line with the evolution of the S 2p spectra, after annealing to 173 K, a shoulder peak with BE of 285.1 eV

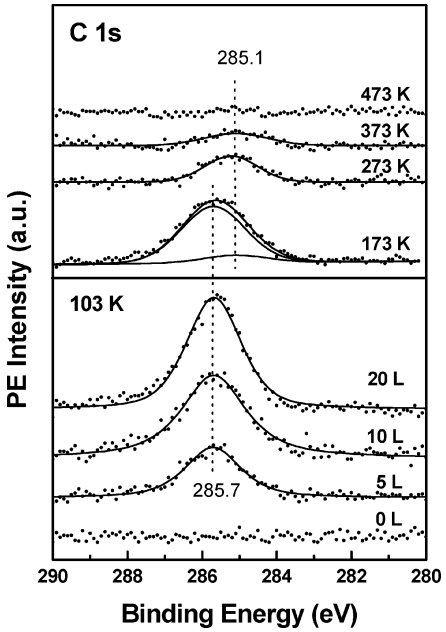

Figure 6. C 1s difference spectra for the adsorption of thiophene on a RQ Ni surface at 103 K, followed by annealing to 173, 273, 373, and 473 K. The C 1s spectrum before thiophene dosage was subtracted from these spectra.

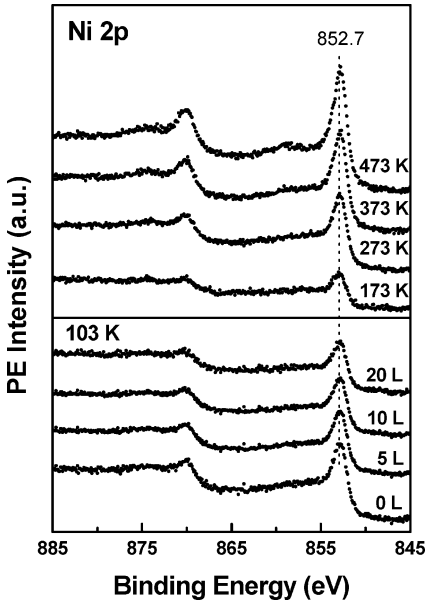

Figure 7. Ni 2p spectra for the adsorption of thiophene on a RQ Ni surface at 103 K, followed by annealing to 173, 273, 373, and 473 K.

emerges, indicative of the formation of a small amount of carbonaceous species due to C−S bond scission. Only annealing to 273 K can lead to the disappearance of the high binding energy peak and the strengthen of the peak at 285.1 eV, which is about 100 K higher than the temperature needed for thiophene dissociation on Raney Ni. The C 1s feature of the carbonaceous species eventually vanishes 473 K.

The Ni 2p and Ni 3p/Al 2p spectra for the adsorption of thiophene on RQ Ni at 103 K, followed by annealing to 173, 273, 373, and 473 K, are illustrated in Figures 7 and 8, respectively. Similar to the spectra of Raney Ni, the intensities of the Ni 2p and Ni 3p/Al 2p peaks are weakened after thiophene adsorption on RQ Ni. After annealing to 173 K, the intensity of the Ni 2p or Ni 3p peak is further attenuated, while it is

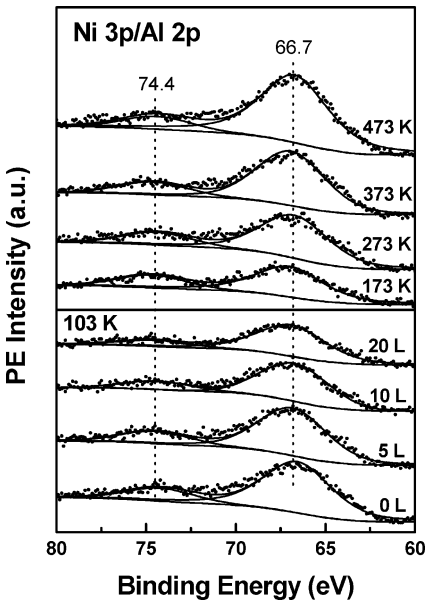

Figure 8. Ni 3p/Al 2p spectra for the adsorption of thiophene on a RQ Ni surface at 103 K, followed by annealing to 173, 273, 373, and 473 K.

increased at higher temperatures. On the contrary, the intensity of Al 2p peak is almost totally recovered at as low as 173 K, indicating no thiophene or other carbonaceous species on alumina.

4. Discussion

A number of experimental and theoretical studies have been undertaken to investigate the surface chemistry of thiophene over Ni single crystals. On Ni(100)[33,34] and Ni(111),[27,35] sulfur is easily removed from the ring with the scission of the C−S bonds. The first layer of thiophene decomposes on Ni(100) even at 90 K, leading to atomic sulfur and a C_4H_3 metallocycle that undergoes further dehydrogenation above 500 K.[34] Stöhr et al.[33] reported that thiophene dissociates on Ni(100) at temperatures as low as 100 K by interacting with 4-fold hollow Ni sites. On the other hand, Imanishi et al.[36] observed molecular adsorption of thiophene on Ni(100) at a coverage of 0.1 ML (monolayer) and a temperature of 43 K. Density functional theory (DFT) calculations identified two adsorption states on Ni(100)—one leaving the molecule intact, while in the other one of the C−S bonds is broken—differing only 0.3 eV in energy agrees with these experimental observations.[37] On Ni(111), substantial C−S bond scission occurs at 100 K and is complete by 150 K, as reported by Huntley et al.[35] Above 150 K, the hydrocarbon intermediate has a metallocycle structure retaining the C_4 framework. On the more open Ni(110) surface, DFT calculations isolated three most stable configurations that all present the aromatic ring parallel to the surface. The most stable adsorption structure of thiophene leads to a thiol via an activated reaction with an energetic barrier of 0.70 eV. The two others can lead to a total dissociation into a C_4H_4 fragment and a sulfur atom, with low barriers.[38]

As compared to well-defined Ni single crystals, the composition and structure of Raney Ni and RQ Ni are more complicated, and consequently the interpretation of the surface behavior of thiophene becomes much more delicate. First, according to Figures 3, 4, 7, and 8, the surfaces of clean Raney Ni and RQ Ni samples are composed of metallic nickel and alumina. The surface compositions of Raney Ni and RQ Ni are calculated from the peak intensity ratios by use of the formula[30]

$$C_x = \frac{n_x}{\sum n_i} = \frac{I_x/S_x}{\sum I_i/S_i}$$

where C is the atomic fraction of the element on the surface, n is the number of atoms, I is the integrated peak area, and S is the atomic sensitivity factor. The Ni 3p and Al 2p peaks are employed for quantification purposes, assuming Shirley background as subtracted in Figures 4 and 8. It is estimated that the surface concentrations of metallic nickel are 67 and 63 mol %, respectively, for Raney Ni and RQ Ni. For comparison, the bulk concentrations of metallic Ni determined by chemical analysis are 82.7 and 79.8 mol %, respectively,[21] suggesting surface aggregation of alumina. For RQ Ni leached under identical conditions, Hu et al.[21] identified the presence of residual Ni_2Al_3 phase in the bulk. Since alkaline leaching of rapidly quenched Ni−Al alloy obeys a shrinking core model,[39] the absence of metallic Al in Figure 8 is supposedly attributed to residual Ni_2Al_3 phase residing in the core of the grains, which is beyond the detection depth of XPS. Second, the metallic Ni in Raney Ni and RQ Ni is nanocrystalline, with diameter of 5∼6 nm and various crystallographic planes being exposed.[21] Third, these samples contain a substantial amount of hydrogen originating from the hydrogen released during alkaline leaching of Al from the Ni−Al alloys.[19] For RQ Ni, it is found that the population of the weakly bound hydrogen is remarkably less than the strongly bound hydrogen, while they are comparable over Raney Ni.[21] After sample cleaning by evacuation at 383 K, the weakly bound hydrogen should have been depleted from the surface, with only the strongly bound hydrogen on the surface. So the adsorption and reaction of thiophene on Raney Ni and RQ Ni can be considered as occurring on the hydrogen preadsorbed polycrystalline Ni−alumina composite surface.

On such surfaces, XPS reveals that the features of metallic Ni and alumina are attenuated at 103 K due to the nonselective adsorption of thiophene. When the sample is annealed to 173 K, the intensity of the Al 2p peak is totally recovered, as shown in Figures 4 and 8 for Raney Ni and RQ Ni, respectively, implying no thiophene and dissociated fragments left on alumina. There are only limited works on the surface chemistry of thiophene on oxides, but they all point to the weak interaction of thiophene with oxides. For example, on polycrystalline ZnO, Jirsak et al.[29] have concluded that thiophene is weakly chemisorbed, and most desorbs at temperatures below 250 K. On γ-Al_2O_3, following thiophene adsorption at 130 K, TPD reveals two peaks with maximum rates of desorption at 175 and ∼220 K. The former peak is assigned to the desorption of multilayer thiophene, while the latter is desorption of weakly chemisorbed thiophene.[40] Thus, recovery of the intensity of the Al 2p peak at ∼173 K for both Raney Ni and RQ Ni is ascribed to preferential desorption of thiophene from alumina.

On the other hand, at such temperature it is conceivable that at least multilayer thiophene on metallic Ni should have desorbed; however, the intensity of the Ni 2p or Ni 3p peak is further weakened, as depicted in Figures 3, 4, 7, and 8. This phenomenon may be rationalized by supposing a three-dimensional island growth mode of thiophene on metallic Ni at 103 K, similar to the physisorption of furan on Ru(0001) at 80 K.[41] Thus, at 103 K there are still uncovered metallic Ni atoms on the surface. Upon annealing to 173 K, the thermal activated diffusion of multilayer thiophene or readsorption of desorbed thiophene occurs, leading to more thiophene molecules directly bonding to metallic Ni, and as a result, the photoemis-

sion features of metallic Ni are weakened. For Raney Ni, the covering of metallic Ni by the dissociated fragments may also contribute to the weakened Ni 2p/3p peaks.

On Raney Ni, thiophene in direct contact with metallic Ni readily decomposes upon thermal annealing to carbonaceous species and atomic sulfur. Figures 1 and 2 demonstrate that the C−S bonds of thiophene have broken at ~173 K on Raney Ni, close to ~150 K on Ni(111),[27] while higher than the temperature on Ni(100).[33,34] It is consistent with the experimental fact that the (111) diffraction peak is the dominant feature in the diffractogram of Raney Ni.[21] From the present study the structure of the surface carbonaceous species cannot be specified; however, by analogy to the configuration on Ni single crystals,[27,33−35,38] it is advisable to assume that it has a metallocycle-like configuration with the sulfur atom in the thiophene ring replaced by a surface Ni atom, which is partly supported by the invariant fwhm of the C 1s peaks before and after S abstraction.

On RQ Ni, however, most thiophene remains intact at 173 K and does not dissociate until 273 K, which is remarkably higher than the temperatures on Ni single crystals and Raney Ni. In a recent work, we found that the unit-cell dimension of nickel in Raney Ni is 0.3525 nm, in agreement with the value for crystalline Ni of 0.352 38 nm, while the unit-cell dimension for RQ Ni is 0.3548 nm, significantly larger than the values of Raney Ni or crystalline Ni.[21] The discrepancy is attributable to the effect of rapid quenching, which leads to atoms in the Ni−Al alloy deviating from their equilibrium positions. It is anticipated that the dissociation of a reacting molecule is possible only if there is a good match between the interatomic distances in the molecule and the atomic arrangement of the superficial metal atoms.[42] The increment of the lattice constant of the RQ Ni sample, as an indication of the increment of the Ni−Ni distance, may be adverse to the scission of the C−S bonds. The rapid quenching technique thus opens a new avenue for designing metallic adsorbents with controllable bonding strength toward thiophene and thiophenic compounds. For example, by further increasing the quenching rate, it is possible to obtain Ni adsorbent on which thiophene does not decompose even at room temperature. The intact thiophene molecules can be removed via supercritical CO_2 extraction,[43] thus simplifying the regeneration of the Ni adsorbent. Moreover, by tailoring the Ni−Ni distance, it is possible to weaken the interaction between the adsorbent and the olefins in gasoline and diesel fuels, which reduces the amount of olefins competitively adsorbed on the adsorbent and gives rise to an improved efficiency in sulfur removal while retaining the octane/cetane number.

Based on the interpretation and arguments presented above, the adsorption and thermal dissociation pathways of thiophene on Raney Ni and RQ Ni are schematically outlined in Figure 9. It is noted that at 473 K only sulfur remains on Raney Ni and RQ Ni in the form of nickel sulfide, while carbonaceous species totally desorbs from the surface. However, on clean Ni(111) the carbonaceous species further decomposes to carbon and hydrogen as the major pathway.[35] It is possible that the dissociation of the carbonaceous species requires more adjacent nickel atoms, while on Raney Ni and RQ Ni they are partitioned by alumina, which blocks this pathway. On the other hand, Huntley et al.[35] also identified that the selectivity to hydrocarbon production can be enhanced by a factor of 3 by predosing the Ni(111) surface with hydrogen before thiophene adsorption. Such a reaction pathway may be also operative on Raney Ni and RQ Ni with strongly bound hydrogen, thus leading to the absence of carbon at 473 K.

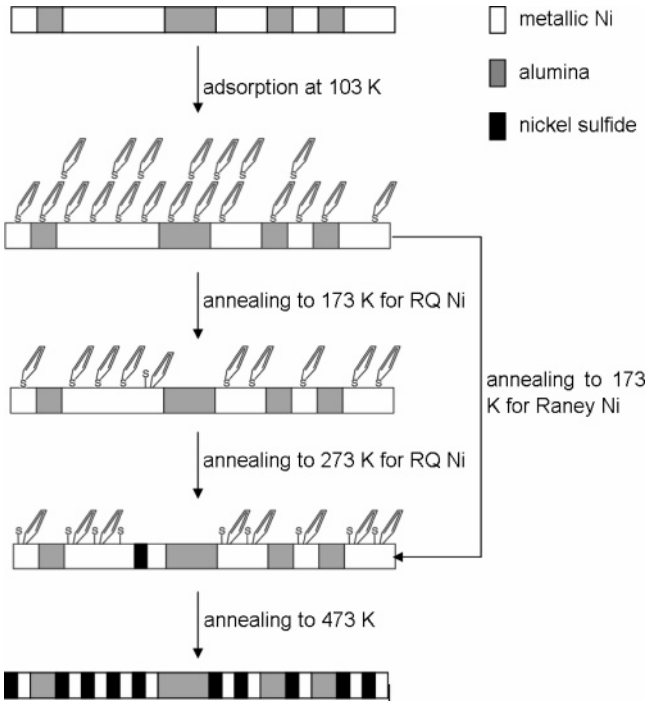

Figure 9. Proposed mechanism for thiophene adsorption and dissociation on Raney Ni and RQ Ni. For clarity, the hydrogen atoms bonding to the samples are not shown.

5. Conclusions

The adsorption and reaction of thiophene on Raney Ni and RQ Ni have been examined. Thiophene molecularly adsorbs on Raney Ni and RQ Ni at 103 K. The molecules on alumina are preferentially desorbed at 173 K, while the dissociation of first-layer thiophene on metallic Ni to a possible metallocycle-like carbonaceous species and atomic sulfur is observed. It is found that the reactivity of metallic Ni toward thiophene is closely related to the preparation history of the pristine Ni−Al alloys. On Raney Ni, sulfur abstraction has been accomplished at 173 K, ~100 K lower than that on RQ Ni, attributable to the increased lattice parameter of Ni crystallites in RQ Ni as compared to that in crystalline Ni or Raney Ni. At higher temperatures, atomic sulfur converts to nickel sulfide, while the metallocycle-like carbonaceous species totally desorbs from both surfaces rather than undergoing further decomposition, presumably due to the existence of alumina and strongly bound hydrogen that alter the reaction pathway dominant on clean Ni single crystals.

Acknowledgment. This work is supported by the State Key Basic Research Development Program (G2000048009), the Natural Science Foundation of China (20203004), and Shanghai (02ZA14006).

References and Notes

(1) Stern, A. C.; Boubel, R. W.; Turner, D. B.; Fox, D. L. *Fundamentals of Air Pollution*, 2nd ed.; Academic Press: New York, 1984.
(2) Bartholomew, C. H.; Agrawal, P. K.; Katzer, J. R. *Adv. Catal.* **1982**, *31*, 135.
(3) Oudar, J. *Catal. Rev.-Sci. Eng.* **1980**, *22*, 171.
(4) Plantenga, F. L.; Leliveld, R. G. *Appl. Catal. A* **2003**, *248*, 1.
(5) Rossini, S. *Catal. Today* **2003**, *77*, 467.
(6) Babich, I. V.; Moulijin, J. A. *Fuel* **2003**, *82*, 67.

(7) Hernández-Maldonado, A. J.; Yang, R. T. *Ind. Eng. Chem. Res.* **2004**, *43*, 1081.
(8) Yang, R. T. *Adsorbents: Fundamentals and Applications*; Wiley: New York, 2003.
(9) Yang, R. T.; Hernández-Maldonado, A. J.; Yang, F. H. *Science* **2003**, *301*, 79.
(10) Wardencki, W.; Staszewski, R. *J. Chromatogr.* **1974**, *91*, 715.
(11) Salem, A. S.; Hamid, H. S. *Chem. Eng. Technol.* **1997**, *20*, 342.
(12) Velu, S.; Ma, X.; Song, C. *Ind. Eng. Chem. Res.* **2003**, *42*, 5293.
(13) Richardeau, D.; Joly, G.; Canaff, C.; Magnoux, P.; Guisnet, M.; Thomas, M.; Nicolaos, A. *Appl. Catal. A* **2004**, *263*, 49.
(14) Garcia, C. L.; Lercher, J. A. *J. Phys. Chem.* **1992**, *96*, 2669.
(15) Hurd, C. D.; Runder, B. *J. Am. Chem. Soc.* **1951**, *73*, 5157.
(16) Pizey, J. S. *Synthetic Reagents*, Vol. 2; Wiley: New York, 1974.
(17) Spera, M. L.; Harman, W. D. *J. Am. Chem. Soc.* **1997**, *119*, 8843.
(18) Lin, H. L. M.Sc. Thesis, Research Institute for Petroleum Processing, Beijing, China, 2002.
(19) Fouilloux, P. *Appl. Catal.* **1983**, *8*, 1.
(20) Freel, J.; Pieters, W. J. M.; Anderson, R. B. *J. Catal.* **1969**, *14*, 247.
(21) Hu, H. R.; Qiao, M. H.; Wang, S.; Fan, K. N.; Li, H. X.; Zong, B. N.; Zhang, X. X. *J. Catal.* **2004**, *221*, 612.
(22) Molnár, Á.; Smith, G. V.; Bartók, M. *Adv. Catal.* **1989**, *36*, 329.
(23) Hashimoto, K. *Mater. Sci. Eng. A* **1997**, *226*−*228*, 891.
(24) Lei, H.; Song, Z.; Tan, D. L.; Bao, X. H.; Mu, X. H.; Zong, B. N.; Min, E. Z. *Appl. Catal. A* **2001**, *214*, 69.
(25) Satterfield, C. N. *Heterogeneous Catalysis in Practice*; McGraw-Hill: New York, 1980.
(26) Wiegand, B. C.; Friend, C. M. *Chem. Rev.* **1992**, *92*, 491.
(27) Schoofs, G. R.; Preston, R. E.; Benziger, J. B. *Langmuir* **1985**, *1*, 313.
(28) Briggs, D.; Seah, M. P. *Practical Surface Analysis*, 2nd ed.; John Wiley & Sons: New York, 1995; Vol. 1, p 113.
(29) Jirsak, T.; Dvorak, J.; Rodriguez, J. A. *J. Phys. Chem. B* **1999**, *103*, 5550.
(30) *Handbook of X-ray Photoelectron Spectroscopy*; Perkin-Elmer Corporation: 1992.
(31) Barrio, V. L.; Arias, P. L.; Cambra, J. F.; Güemez, M. B.; Campos-Martin, J. M.; Pawelec, B.; Fierro, J. L. G. *Appl. Catal. A* **2003**, *248*, 211.
(32) Gelius, U.; Allan, C. J.; Johansson, G.; Siegbahn, H.; Allison, D. A.; Siegbahn, K. *Phys. Scr.* **1971**, *3*, 237.
(33) Stöhr, J.; Kollin, E. B.; Fischer, D. A.; Hastings, J. B.; Zaera, F.; Sette, F. *Phys. Rev. Lett.* **1985**, *55*, 1468.
(34) Zaera, F.; Kollin, E. B.; Gland, J. L. *Langmuir* **1987**, *3*, 555.
(35) Huntley, D. R.; Mullins, D. R.; Wingeier, M. P. *J. Phys. Chem.* **1996**, *100*, 19620.
(36) Imanishi, A.; Yagi, S.; Kitajima, Y.; Ohta, T. *J. Electron Spectrosc. Relat. Phenom.* **1996**, *80*, 151.
(37) Mittendorfer, F.; Hafner, J. *Surf. Sci.* **2001**, *492*, 27.
(38) Morin, C.; Eichler, A.; Hirschl, R.; Sautet, P.; Hafner, J. *Surf. Sci.* **2003**, *540*, 474.
(39) Hu, H. R.; Qiao, M. H.; Pei, Y.; Fan, K. N.; Li, H. X.; Zong, B. N.; Zhang, X. X. *Appl. Catal. A* **2003**, *252*, 173.
(40) Quigley, W. W. C.; Yamamoto, H. D.; Aegerter, P. A.; Simpson, G. J.; Bussell, M. E. *Langmuir* **1996**, *12*, 1500.
(41) Yan, F. Q.; Qiao, M. H.; Wei, X. M.; Liu, Q. P.; Deng, J. F.; Xu, G. Q. *J. Chem. Phys.* **1999**, *111*, 8068.
(42) Balandin, A. A. *Z. Phys. Chem.* **1929**, *132*, 289.
(43) Vradman, L.; Herskowitz, M.; Korin, E.; Wisniak, J. *Ind. Eng. Chem. Res.* 2001, *40*, 1589.